BIOCHEMISTRY
including biophysical chemistry & molecular biology

Article

pubs.acs.org/biochemistry

Kinetic Properties of an RNA Enzyme That Undergoes Self-Sustained Exponential Amplification

Antonio C. Ferretti and Gerald F. Joyce*

Departments of Chemistry and Molecular Biology and The Skaggs Institute for Chemical Biology, The Scripps Research Institute, 10550 North Torrey Pines Road, La Jolla, California 92037, United States

ABSTRACT: A special class of biochemical reactions involves a set of enzymes that generate additional copies of themselves and transfer heritable information from parent to progeny molecules, thus providing the basis for genetics and Darwinian evolution. Such a process has been realized with a pair of self-replicating RNA enzymes that undergo exponential amplification at a constant temperature. Exponential growth requires that the rate of production of new enzymes be directly proportional to the existing concentration of enzymes, which is the case for this system and provides a doubling time of ∼20 min. However, the catalytic rate of the underlying enzymes is ∼100-fold faster than the observed rate of replication. As in biological replication, other aspects of the system limit the generation time, chiefly the propensity of the substrate molecules to form nonproductive complexes that limit their availability for replication. An analysis of this and other kinetic properties of the self-replicating RNA enzymes reveals how exponential amplification is achieved and how the rate of amplification might be increased.

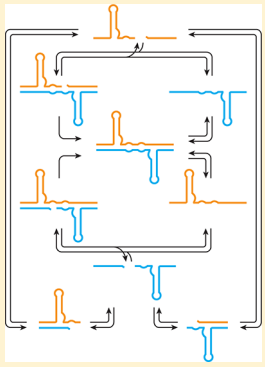

The development of self-replicating chemical systems that undergo exponential amplification has been an important research goal since von Kiedrowski's demonstration of a self-replicating hexadeoxynucleotide.[1] Following that seminal work, other self-replicating systems have been devised, including ones based on nucleic acids,[2−5] peptides,[6−8] small organic molecules,[9,10] and more complex architectures such as DNA nanoscale motifs[11] and DNA crystals.[12] These systems typically entail a template that directs the joining of two substrates to form a product that is identical to the template. Autocatalysis occurs when the product also can function as a template, directing the formation of additional products. Exponential growth, however, is usually not observed in these systems because amplification is limited by slow dissociation of the template−product complex.[13,14]

Recently, a self-replicating system that is based on an RNA enzyme with RNA ligase activity[15] and can undergo sustained exponential growth at a constant temperature was described.[16] The enzyme catalyzes the template-directed joining of two RNA substrates to form another copy of itself. The template−product complex dissociates in a non-rate-limiting manner, allowing amplification to proceed indefinitely so long as additional substrates are provided. The enzyme usually is made to operate as a cross-replicating pair, whereby two enzymes direct each other's synthesis from a total of four component substrates (Figure 1).[17] One enzyme, E, catalyzes the joining of two substrates, A′ and B′, to form the other enzyme, E′. Similarly, E′ catalyzes the joining of A and B to form E. The joining reaction catalyzed by either E or E′ results in formation of a 3′,5′-phosphodiester linkage between the two corresponding substrates, with concomitant release of inorganic pyrophosphate. No proteins or other informational macromolecules are required for replication, and in this sense, the system is said to be self-sustaining.

In the system of self-replicating RNA enzymes, heritable information can be transferred from parent to progeny molecules in the form of particular sequences located within two template regions of the enzyme and corresponding complementary regions of the substrates. Novel variation can arise because of recombination between these two regions, and different genetic variants can be made to encode corresponding functional variants of the enzyme. By combining exponential amplification of heritable information, the opportunity for mutation, and selection of advantageous phenotypes, the system is capable of undergoing Darwinian evolution in a self-sustained manner.[16,18]

The self-replicating system also has been used as a tool to measure the concentration of various target molecules.[19,20] In this format, an aptamer domain is linked to the catalytic domain of the enzyme such that, upon binding its cognate ligand, the aptamer adopts a defined structure that results in activation of the enzyme. The exponential growth rate of the enzyme reflects the concentration of the ligand relative to the K_d of the aptamer−ligand interaction. This configuration allows the real-time, quantitative detection of various target molecules, analogous to quantitative polymerase chain reaction, but applicable to small-molecule and protein ligands.

The exponential growth rate of the self-replicating RNA enzymes is ∼0.03 min^{-1}, corresponding to a doubling time of ∼20 min.[16] It would be advantageous to increase this rate to allow more rapid self-sustained evolution and more rapid detection of target ligands. To guide these efforts, this study sought to understand the kinetic properties of the RNA-

Received: December 10, 2012
Revised: January 22, 2013
Published: January 23, 2013

dx.doi.org/10.1021/bi301646n | *Biochemistry* 2013, 52, 1227−1235

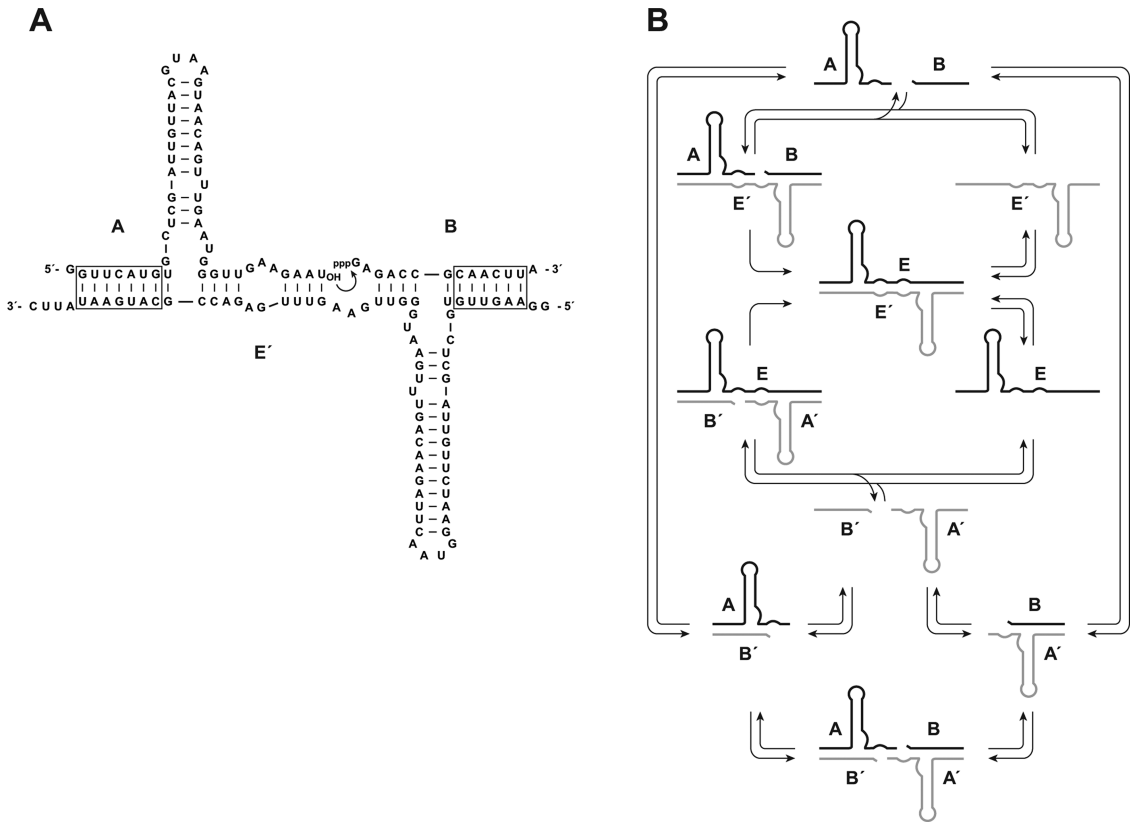

Figure 1. Self-replicating RNA enzymes. (A) Sequence and secondary structure of enzyme E′ and its substrates A and B. The curved arrow indicates the site of ligation for the formation of the partner enzyme E, which similarly reacts with substrates A′ and B′ to form E′. Boxed regions indicate paired nucleotides that can vary in sequence. (B) Scheme for cross-replication of E (black) and E′ (gray), including the equilibrium between free substrates and the A·B′, A′·B, and B′·A·A′·B complexes.

catalyzed exponential amplification system. Such insights also may be useful in increasing the complexity of the synthetic evolving system, which presently is limited to a few thousand variants and therefore has little capacity for inventive evolution. Two important constraints on the genetic complexity of the system are the modest fidelity of replication and the sequestration of reaction materials within nonproductive complexes. The issue of replication fidelity has been addressed in another recent study.[18] The study presented here provides a better understanding of the nonproductive complexes and suggests how they might be overcome.

EXPERIMENTAL PROCEDURES

Materials. DNA templates were synthesized using an Applied Biosystems (Foster City, CA) Expedite 8909 automated DNA/RNA synthesizer. Nucleoside phosphoramidites were purchased from Glen Research (Sterling, VA). *Thermus aquaticus* DNA polymerase and histidine-tagged T7 RNA polymerase were expressed and purified as previously described.[21,22] Nucleoside and deoxynucleoside 5′-triphosphates were purchased from Sigma-Aldrich (St. Louis, MO); Antarctic phosphatase and T4 polynucleotide kinase were from New England Biolabs (Ipswich, MA), and [γ-^{32}P]ATP (6 μCi/pmol) and [α-^{32}P]ATP (3 μCi/pmol) were from Perkin-Elmer (Waltham, MA).

Preparation of Oligonucleotides. Enzymes E and E′ were prepared by in vitro transcription of corresponding synthetic DNA templates. Substrates A and A′ were obtained by site-specific cleavage of E and E′, respectively, using *Escherichia coli* M1 RNA and an external guide RNA to generate products terminating in a 2′- and 3′-hydroxyl.[23] The external guide RNAs had sequences 5′-CGUAAGUUGCGGUCUCACCA-3′ and 5′-AUAUUCAUGCGGUCUCACCA-3′ for A and A′, respectively (region of hybridization underlined). Substrates B and B′ were prepared by in vitro transcription, with a hammerhead ribozyme appended to their 3′ termini to provide a homogeneous 3′ end upon self-cleavage during transcription. The transcribed RNAs had sequences 5′-GAGACCGCAACUUA·UACGGAAACGUACUGAUGAGGCCGAAAGGCCGAAAAGUUG-3′ and 5′-GAGACCGCAUGAAUAUUC·UACGGAAACGUACUGAUGAGGCCGAAAGGCCGAAAAUAUUC-3′ for B and B′, respectively (hammerhead pairing underlined; cleavage site indicated by a dot). Substrates A and A′ were 5′-^{32}P-labeled by dephosphorylation using Antarctic phosphatase, incubation at 65 °C for 5 min to inactivate the phosphatase, and phosphorylation using T4 polynucleotide kinase and [γ-^{32}P]ATP. Substrates B and B′ were internally labeled by conducting in vitro transcription in the presence of [α-^{32}P]ATP.

Determination of Reaction Rates and Equilibrium Constants. All reactions were conducted in the presence of 25 mM $MgCl_2$ and 50 mM EPPS (pH 8.5) at 44 °C. Aliquots were removed at various times and reactions quenched by adding a solution containing 8 M urea and Na_2EDTA in 3-fold excess over Mg^{2+}. Substrates and products were separated by denaturing polyacrylamide gel electrophoresis (PAGE) and quantitated using a PharosFX molecular imager (Bio-Rad, Hercules, CA).

dx.doi.org/10.1021/bi301646n | *Biochemistry* 2013, 52, 1227−1235

Determination of Michaelis–Menten Parameters. The component reactions, A + B → E and A′ + B′ → E′, were conducted under enzyme-excess, single-turnover conditions using trace radiolabeled amounts of the substrate being evaluated (<5 nM for A or A′ and 20 nM for B or B′), saturating concentrations of the other substrate (15 μM), and various concentrations of the enzyme that spanned K_M. The reactions were initiated by mixing a solution containing the radiolabeled substrate with a solution containing the other substrate and enzyme, both at 44 °C. First-order rate constants, k_{obs}, were obtained from a plot of fraction reacted versus time, fitting the data to a single-exponential equation:

$$F(t) = F_{max}(1 - e^{-k_{obs}t}) \quad (1)$$

where $F(t)$ is the fraction reacted at time t and F_{max} is the maximal extent of the reaction. Values for k_{cat} and K_M were obtained from a plot of k_{obs} versus [E] (or [E′]), fitting the data to the Michaelis–Menten equation:

$$k_{obs} = k_{cat}[E]/(K_M + [E]) \quad (2)$$

Determination of Dissociation Rates by Pulse–Chase Experiments. A mixture containing 0.5 μM 5′-^{32}P-labeled E, 1 μM E′, 25 mM $MgCl_2$, and 50 mM EPPS (pH 8.5) was equilibrated first at 23 °C for 20 min and then at 44 °C for 30 min. A chase solution was added that also had been equilibrated at 44 °C for 30 min and contained a large excess of unlabeled E (final concentration of 30 μM), 25 mM $MgCl_2$, and 50 mM EPPS (pH 8.5). Aliquots were withdrawn at various times and subjected to gel-shift analysis in a 10% nondenaturing polyacrylamide gel containing 12 mM $MgCl_2$, 2 mM Na_2EDTA, and 90 mM Tris-borate (pH 8.3). The fraction of shifted material versus time was fit to a single-exponential equation, and k_{dissoc} was calculated as the exponential decay rate. The same procedure was applied to a mixture containing 0.5 μM α-^{32}P-labeled B (or B′) and 1 μM A′ (or A), chasing with 30 μM unlabeled B (or B′). In that case, the labeled material was fully shifted prior to the chase, but >90% was displaced within 30 s.

Determination of the K_d of the E·E′ Complex. Gel-shift analysis was conducted by employing trace amounts (<1 nM) of 5′-^{32}P-labeled E and various concentrations of unlabeled E′, which were equilibrated at 23 °C for 20 min and then at 44 °C for 1 h. The material was analyzed by nondenaturing polyacrylamide gel electrophoresis, as described above. The fraction of labeled E that bound to E′ was determined as a function of [E′], and the data were fit to a saturation plot, from which K_d was determined.

Determination of the K_d of the A·B′ and A′·B Complexes. The component reactions were monitored using the same protocol that was used for determining the Michaelis–Menten parameters, employing trace amounts of 5′-^{32}P-labeled A (or A′) and various concentrations of unlabeled B′ (or B), which first were allowed to reach equilibrium and then were mixed with B and E′ (or B′ and E). Values for k_{obs} were determined as described above, and a plot of k_{obs} versus [E′] (or [E]) was used to determine a value for K_M^{app} in each instance. The K_M^{app} values were related to k_{cat} and K_M that had been determined in the absence of competing substrate to provide an estimate of K_d:

$$k_{obs} = k_{cat}[E']/([E'] + K_M^{app}) = k_{cat}[E']/\{[E'] + K_M[1 + ([B]/K_d)]\} \quad (3)$$

K_d was determined separately for two different concentrations of the competing substrate for each of the two component reactions.

Self-Replication Reactions. Reactions were initiated by combining an equilibrated solution containing 5′-^{32}P-labeled A, 5′-^{32}P-labeled A′, E, and E′ with a second equilibrated solution containing B and B′, both solutions also containing 25 mM $MgCl_2$ and 50 mM EPPS (pH 8.5). Unless otherwise stated, the reactions employed A, A′, B, and B′ (5 μM each) and E and E′ (0.1 μM each) and were conducted at 44 °C. The reaction mixtures were sampled at various times, and the products were separated by PAGE to determine the yield of radiolabeled E and E′. The data were fit to the logistic growth equation:

$$[E]_t = a/(1 + be^{-ct}) \quad (4)$$

where $[E]_t$ is the concentration of E (or E′) at time t, a is the maximal extent of growth, b is the degree of sigmoidicity, and c is the exponential growth rate. The pseudo-first-order rate constant for the initial phase of the reaction was obtained from the derivative of the logistic growth equation, which at $t = 0$ is

$$k_{obs} = abc/[[E]_0(1 + b^2)] \quad (5)$$

The initial rate of reaction also was measured directly for various starting concentrations of both E and E′, collecting data over the first 10% of the reaction. These data were fit to a linear plot, rejecting any data for which the linear regression coefficient was <0.98.

Kinetic Modeling. A model was constructed on the basis of Figure 1B, incorporating the exponential amplification profiles for E and E′ shown in Figure 2A and the experimentally determined K_d values for the E·E′, A·B′, and A′·B complexes. The starting concentrations of the B and B′ substrates were adjusted for their maximal extents of reaction, which were 3.9 and 2.9 μM, respectively. The total concentration of each substrate over time was calculated by subtracting the concentration of the product from the initial concentration of the substrate. The concentrations of the E·E′, A·B′, and A′·B complexes were calculated from the experimentally determined K_d values, considering the relevant equilibrium and solving the quadratic equation, for example, for the A·B′ complex:

$$[A\cdot B'] = \{K_d^{A\cdot B'} + [A]_{tot} + [B']_{tot} - [(-K_d^{A\cdot B'} - [A]_{tot} - [B']_{tot})^2 - 4[A]_{tot}[B']_{tot})^{0.5}\}/2 \quad (6)$$

where $[A]_{tot}$ and $[B']_{tot}$ are the total concentrations of A and B′, respectively.

RESULTS

The system of self-replicating RNA enzymes involves two component reactions: A + B → E and A′ + B′ → E′ (Figure 1). These reactions first were studied in isolation to determine the relevant underlying catalytic parameters. Each component reaction involves binding of two substrates to the enzyme, followed by a chemical step that is thermodynamically highly favorable and essentially irreversible, and finally dissociation of the E·E′ complex to complete the catalytic cycle. Non-rate-limiting product release is essential for exponential amplification.

The A and A′ substrates bind to the E′ and E enzymes, respectively, through three discontinuous regions of Watson–Crick pairing (Figure 1A). Two of these regions involve 4 bp of defined sequence, and the third involves 6–7 bp of variable

dx.doi.org/10.1021/bi301646n | Biochemistry 2013, 52, 1227–1235

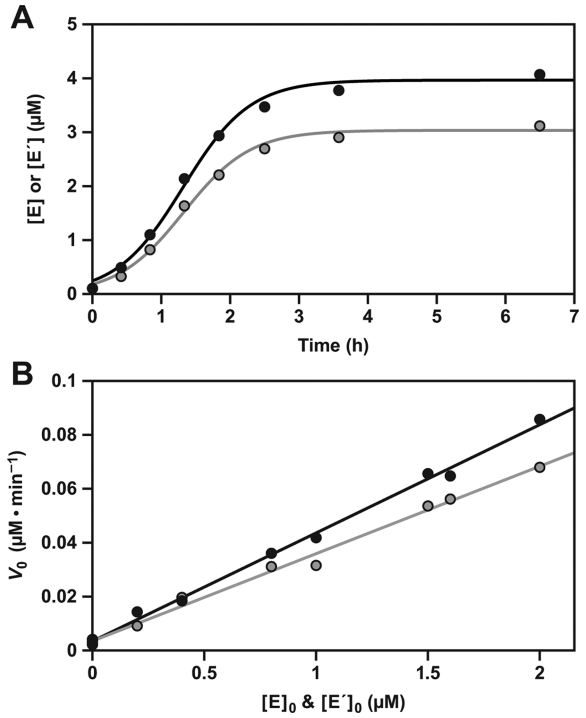

Figure 2. Exponential amplification of the replicating RNA enzymes. (A) Time course of amplification, starting with E and E′ (0.1 μM each), A, A′, B, and B′ (5 μM each), and 25 mM $MgCl_2$, conducted at pH 8.5 and 44 °C. The data were fit to the logistic growth equation, which gave an exponential growth rate of 0.034 min^{-1} for the production of both E (black) and E′ (gray). The pseudo-first-order rate constant was calculated from the derivative of the logistic growth equation, applied to the first 15% of the reaction, which gave observed rates of 0.037 and 0.025 min^{-1} for the production of E and E′, respectively. (B) Initial rates of reaction (V_0) for the production of both E and E′, under the same conditions described above, but with various starting concentrations of the two enzymes. A linear fit to the data gave exponential growth rates of 0.040 and 0.032 min^{-1} for the production of E and E′, respectively, and rates for the spontaneous reaction in the absence of enzymes of 3.5×10^{-9} M min^{-1} for both E and E′.

sequence. The B and B′ substrates bind to their respective enzymes through two discontinuous regions of Watson–Crick pairing, one involving 4 bp of defined sequence and the other involving 6–7 bp of variable sequence. The bound substrates also may engage in tertiary interactions with the enzyme, for example, through interactions involving the central stem–loop region of A and A′. The ligated product binds to the enzyme through five discontinuous regions of Watson–Crick pairing, as well as potential tertiary interactions.

When all four substrates are present in the same mixture, there is the opportunity to form A·B′ and A′·B complexes because of the partial complementarity of these molecules (Figure 1B). Such complexes are expected to reduce the effective concentration of the substrates and therefore reduce the efficiency of the RNA-catalyzed reaction. The four substrates also can form a B′·A·A′·B complex in which the A and A′ components, likely preassociated as A·B′ and A′·B complexes, respectively, bind to each other through a central region of 4 bp. This tetramolecular complex has been shown to have a low level of catalytic activity, resulting in the spontaneous formation of E and E′ molecules that then undergo autocatalytic amplification.[19]

The complete self-replication reaction involves reciprocal synthesis of E and E′ from the four component substrates. A plot of enzyme concentration versus time has a sigmoidal shape (Figure 2A), indicative of exponential growth limited by the fixed concentration of substrates.[16] The reactions are typically performed in the presence of 25 mM $MgCl_2$ at pH 8.5 and 44 °C, resulting in an exponential growth rate of 0.03 min^{-1}. The maximal extent of the reaction is typically 80% for substrates that are prepared by in vitro transcription. However, another study has shown that a maximal extent of >90% can be achieved when both the B and B′ substrates are prepared synthetically,[24] which may be indicative of sequence heterogeneity at the 5′ end of the transcribed materials.[25,26] There is some degradation of the RNA during the course of the reaction, which occurs at a constant rate of ~5% h^{-1}. The degradation rate is similar for the unreacted substrates and ligated products and thus has little effect on the determination of the fraction reacted.

A formal demonstration of exponential growth is obtained by measuring the initial rate of reaction as a function of the starting concentration of the enzyme, fitting the data to the equation

$$(d[E]/dt)_0 = (k_{auto}[E]_0^{\,p}) + k_{spont} \quad (7)$$

where the initial rate, $(d[E]/dt)_0$, is proportional to the starting enzyme concentration, $[E]_0$, raised to the reaction order p. A plot of $(d[E]/dt)_0$ versus $[E]_0^{\,p}$ has a slope equal to the autocatalytic rate constant, k_{auto}, and a y-intercept equal to the rate of reaction in the absence of enzyme, k_{spont}. Exponential growth occurs when the reaction order is 1.0.[13] Data were obtained for starting concentrations of both E and E′ of 0–2 μM and fit well to a plot with a reaction order of 1.0 (r = 0.998, 0.996), confirming exponential growth (Figure 2B). The autocatalytic rate constants are 0.040 and 0.032 min^{-1} for the production of E and E′, respectively, coinciding with the overall exponential growth rate of 0.03 min^{-1}. The efficiency of replication, k_{auto}/k_{spont}, is ~10^7 M^{-1}.

Steady-State Catalytic Parameters. Michaelis–Menten parameters were determined for each of the two component reactions, measured under enzyme-excess, single-turnover conditions for each of the two substrates (Figure 3). These reactions employed a trace concentration of the substrate being evaluated, a saturating concentration of the other substrate, and various concentrations of the enzyme that spanned K_M. The values for k_{cat} all are in the range of 2–5 min^{-1}, with the E-catalyzed reaction being ~2-fold faster than the E′-catalyzed reaction (Table 1). These rates are ~100-fold faster than the observed rate of reaction for the complete self-replication system (Figure 2A), suggesting that other steps in the replication cycle are rate-limiting.

The K_M values for the four substrates, also determined under enzyme-excess, single-turnover conditions, are in the range of 1–8 μM, with the K_M values for A and A′ being several-fold higher than those for B and B′ (Table 1). This disparity has been noted previously[4,16] and may reflect the more complex folded structure of the A and A′ substrates, which results in a smaller fraction of these molecules adopting the properly folded state.

Dissociation of the E·E′ Complex. The rate of dissociation of the E·E′ complex was determined by pulse–chase experiments in which radiolabeled E and unlabeled E′ first were allowed to bind at equilibrium, then a large excess of unlabeled E was added, and aliquots were withdrawn at various times to determine the fraction of radiolabeled E that remained

dx.doi.org/10.1021/bi301646n | Biochemistry 2013, 52, 1227–1235

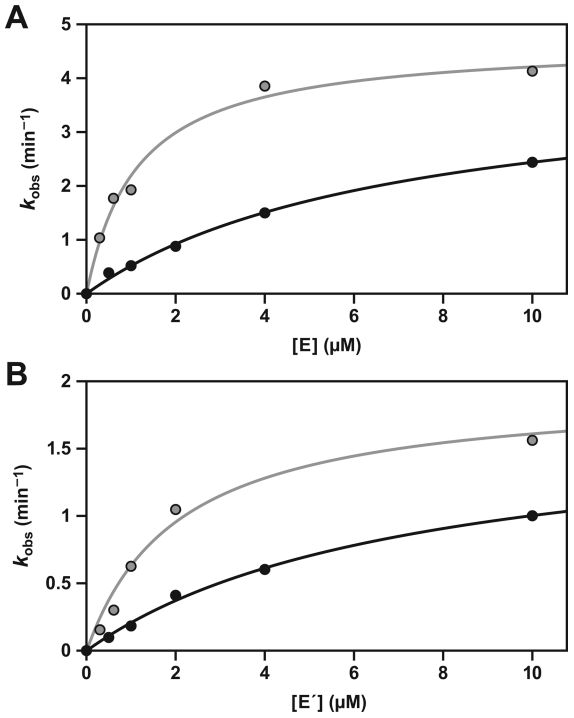

Figure 3. Catalytic activity of the replicating RNA enzymes in the component ligation reactions, conducted under enzyme-excess, single-turnover conditions. (A) E-catalyzed ligation of A′ (black) or B′ (gray), (B) E′-catalyzed ligation of A (black) or B (gray), all with saturating concentrations of the other substrate and various concentrations of enzyme. The data were fit to the Michaelis–Menten equation: $k_{obs} = k_{cat}[E]/(K_M + [E])$.

Table 1. Michaelis–Menten Parameters for the Component Ligation Reactions

enzyme	substrate	k_{cat} (min^{-1})	K_M (μM)
E	A′	4.1 ± 0.3	7.0 ± 0.9
E	B′	4.7 ± 0.2	1.1 ± 0.2
E′	A	1.7 ± 0.1	7.4 ± 1.1
E′	B	1.9 ± 0.2	2.1 ± 0.5

bound to E′. The data fit well to a single-exponential decay, giving a value for k_{dissoc} of 0.21 min^{-1} at 44 °C (Figure 4A). This value is similar to that reported previously for a less optimized form of the enzyme[17] and is ~10-fold smaller than the value for k_{cat}, as described above. Thus, multiple turnovers of the two component reactions are limited by the rate of product release, even though this is not the case for the complete self-replication system, which has an even slower observed rate.

The K_d of the E·E′ complex was determined by gel-shift analysis, giving a value of 16 nM at 44 °C (Figure 4B). The self-replication reaction typically employs a starting concentration of 5 μM for each of the four substrates and 0.01–0.1 μM for each of the two enzymes and results in the production of ~4 μM for each of the two enzymes at the maximal extent. Thus, throughout most of the course of the reaction, the concentrations of the two enzymes are substantially in excess of the K_d of the E·E′ complex, suggesting that the majority of enzyme molecules are engaged in this complex rather than being free in solution. However, the dissociation rate of this complex is sufficiently fast that free E and E′ molecules are continually made available to bind additional substrates. The

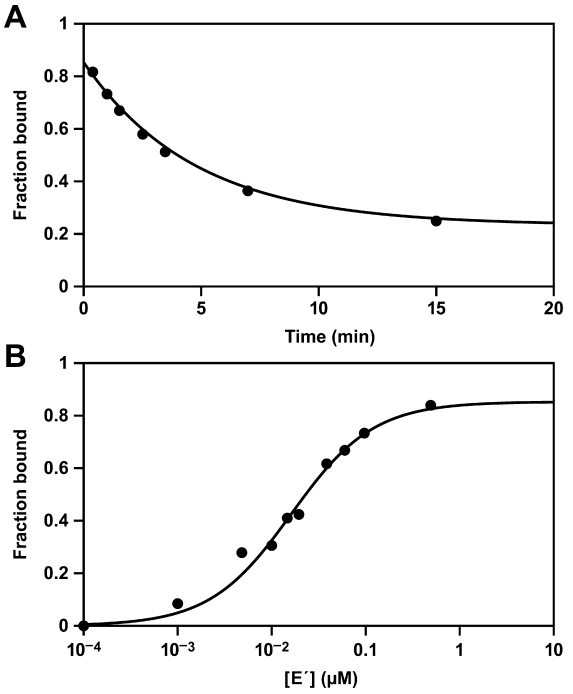

Figure 4. Stability of the E·E′ complex. (A) The rate of dissociation of the E·E′ complex was determined by pre-equilibrating radiolabeled E and unlabeled E′ and then chasing with a large excess of unlabeled E. The fraction of labeled E that remained bound to E′ at various times was determined by gel-shift analysis, and the data were fit to an exponential decay equation. (B) The K_d of the E·E′ complex was determined by gel-shift analysis, measuring the fraction of labeled E that bound to various concentrations of unlabeled E′. The data were fit to a saturation plot: $F_{bound} = [E']/(K_d + [E'])$.

calculated rate of association of the E·E′ complex is given by the equation $k_{assoc} = k_{dissoc}/K_d = 1.3 \times 10^7$ M^{-1} min^{-1}. This rate is only ~10-fold slower than the rate of helical nucleation of complementary RNA molecules under similar reaction conditions.[27,28]

Dissociation of the A·B′ and A′·B Complexes. The rates of dissociation of the A·B′ and A′·B complexes are too fast to measure reliably using pulse–chase methods, with >90% of the labeled material being displaced within 30 s, corresponding to a dissociation rate of >4 min^{-1}. Gel-shift analyses also proved to be unreliable because of the difficulty in preventing dissociation of these complexes during nondenaturing gel electrophoresis, even when performed at a low temperature. Instead, a strategy was devised to measure the rate of ligation in the presence of varying amounts of one of the competing substrates. The A + B → E reaction was conducted in the presence of varying amounts of B′, and the A′ + B′ → E′ reaction was conducted in the presence of varying amounts of B. The K_d values for the A·B′ and A′·B complexes were determined by quantitative analysis of the competitive inhibition (see Experimental Procedures).

The calculated K_d values for the A·B′ and A′·B complexes are 0.058 and 0.16 μM, respectively (Figure 5). These values indicate that in the complete self-replication system most of the substrate molecules are present as nonproductive complexes, rather than being free in solution. If the association rates of the A·B′ and A′·B complexes are similar to the association rate of the E·E′ complex, then the dissociation rates of the A·B′ and A′·B complexes would be ~1 min^{-1}. The attempted pulse–

dx.doi.org/10.1021/bi301646n | *Biochemistry* 2013, 52, 1227–1235

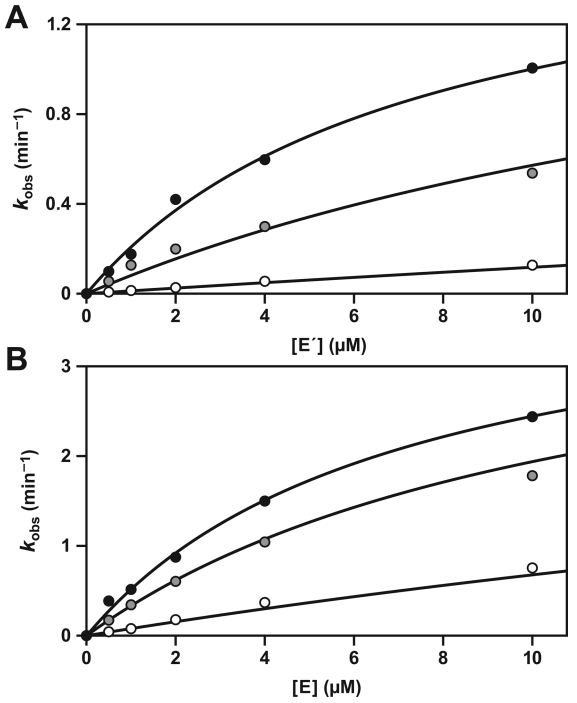

Figure 5. Stability of the A·B′ and A′·B complexes. (A) E′-catalyzed ligation of A and B in the presence of no B′ (black), 0.1 μM B′ (gray), or 1 μM B′ (white). (B) E-catalyzed ligation of A′ and B′ in the presence of no B (black), 0.1 μM B (gray), or 1 μM B (white). Various enzyme concentrations were used. The data were fit to eq 3 (see Experimental Procedures) to obtain the K_d of the A·B′ and A′·B complexes.

chase experiments indicate that these rates are several-fold faster, close to the rate of helical nucleation of RNA duplexes. In any case, dissociation of the A·B′ and A′·B complexes would not be rate-limiting for the complete self-replication system. Rather, it appears that the observed rate of reaction in the complete system is limited by the concentrations of free substrates. On the basis of total substrate concentrations of 5 μM each and the K_d values of the nonproductive complexes, the concentrations of free substrates would be only 0.5 μM for A and B′ and 0.8 μM for A′ and B, which are substantially below the K_M of the corresponding enzyme–substrate complexes.

Considering the free rather than the total concentrations of substrates, the calculated rates of the two component reactions are given by

$$k_{obs}^{E} = (k_{cat}[A'][B'])/(K_M^{A'}K_M^{B'} + [A']K_M^{B'} + [B']K_M^{A'} + [A'][B']) = 0.14\ \text{min}^{-1} \quad (8a)$$

$$k_{obs}^{E'} = (k_{cat}[A][B])/(K_M^{A}K_M^{B} + [A]K_M^{B} + [B]K_M^{A} + [A][B]) = 0.03\ \text{min}^{-1} \quad (8b)$$

where k_{obs}^{E} and $k_{obs}^{E'}$ are the rates of the E- and E′-catalyzed reactions, respectively. The calculated rate of the slower E′-catalyzed reaction closely matches the observed rate of the complete self-replication system, which is ~0.03 min^{-1} (Figure 2A).

Replication with Varying Initial Substrate Concentrations. To explore the role of the nonproductive complexes in reducing the concentrations of free substrates and thereby limiting the rate of self-replication, reactions were conducted using various initial concentrations of one or two substrates, while maintaining the initial concentration of 5 μM of each of the other substrates. When the concentration of A was progressively increased from 5 to 40 μM, the rate of the A′ + B′ → E′ reaction progressively declined (Figure 6A). This is explained by the higher concentrations of A favoring formation of the A·B′ complex, thereby reducing the concentration of free B′ that is available to react with A′. In contrast, the rate of the A + B → E reaction was nearly unchanged as the concentration of A was increased. The higher concentrations of A, in excess of the concentration of B′, might be expected to increase the rate of production of E. However, the concentration of free B remains limiting, and the decreased rate of production of E′ reduces the amount of catalyst available to drive the production of E.

The results were analogous when the concentration of B was increased from 5 to 40 μM, while maintaining a concentration of 5 μM of each of the other three substrates. This manipulation caused the rate of the A′ + B′ → E′ reaction to be reduced, while the rate of the A + B → E reaction was unchanged (Figure 6B). However, increasing the concentration of B to ≥10 μM resulted in an increased maximal extent of reaction for the production of E, reaching >95%. This is consistent with the hypothesis that a fraction of the in vitro-transcribed B molecules are unreactive, with the large excess of B compensating for this deficiency.

Next, the concentrations of both A and A′ were increased from 5 to 40 μM, while maintaining the concentrations of B and B′ at 5 μM (Figure 6C). This resulted in slightly increased rates of production of both E and E′ when the concentrations of A and A′ were increased to 10 μM but decreased rates of production when the concentrations of A and A′ were further increased to 20–40 μM. There are two competing effects at play. Increasing the concentrations of A and A′ results in increased levels of saturation of the corresponding enzymes but also results in increased levels of formation of the nonproductive A·B′ and A′·B complexes. The K_M values for A and A′ are 7.7 and 6.7 μM, respectively. Concentrations of A and A′ in excess of B′ and B, respectively, are available to bind to the corresponding enzymes, but when these excess concentrations reach saturation, they no longer provide a benefit with regard to the observed rate of reaction. They do, however, continue to enhance the rate of formation of the nonproductive complexes, thus reducing the availability of both the B and B′ substrates.

Similar results were obtained when the concentrations of both B and B′ were increased from 5 to 40 μM, while maintaining the concentrations of A and A′ at 5 μM (Figure 6D). There was a modest increase in the rates of production of both E and E′ when the concentrations of B and B′ were increased to 10 μM but decreased rates of production when the concentrations of B and B′ were further increased to 20–40 μM.

When the concentrations of both A and B′ were increased from 5 to 40 μM, while maintaining the concentrations of A′ and B at 5 μM, the rates of production of both E and E′ increased progressively (Figure 6E). At 40 μM A and B′, the exponential growth rate was 0.07 min^{-1}, which is the fastest ever observed with this system, corresponding to a doubling time of ~10 min. The elevated concentrations of both A and B′ result in an increased concentration of the nonproductive A·B′ complex and increased concentrations of free A and B′ substrates, the latter contributing to a faster rate of reaction. Because of the A + B′ ⇆ A·B′ equilibrium, there is a square-root relationship between the increase in the total concen-

dx.doi.org/10.1021/bi301646n | *Biochemistry* 2013, 52, 1227–1235

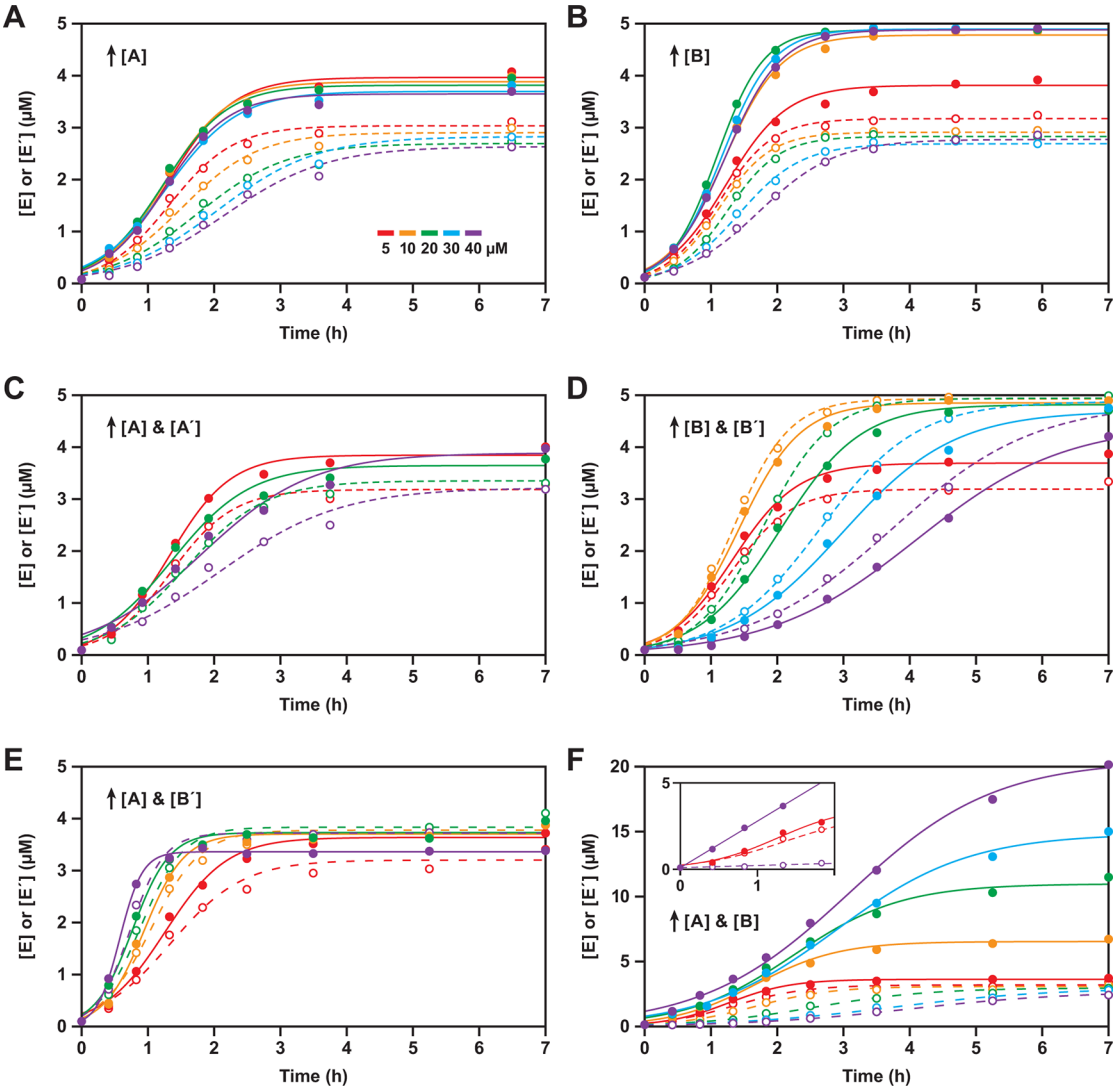

Figure 6. Exponential amplification conducted in the presence of unbalanced concentrations of the four substrates. Unless otherwise stated, all reactions employed E and E′ (0.1 μM each), A, A′, B, and B′ (5 μM each), and 25 mM $MgCl_2$ and were conducted at pH 8.5 and 44 °C. The starting concentrations of one or two substrates were increased from 5 μM (red) to 10 μM (orange), 20 μM (green), 30 μM (blue), or 40 μM (violet). The data were fit to the logistic growth equation, with solid and dashed lines indicating the production of E and E′, respectively: (A) increasing [A], (B) increasing [B], (C) increasing [A] and [A′], (D) increasing [B] and [B′], (E) increasing [A] and [B′], and (F) increasing [A] and [B]. For the sake of clarity, not all concentrations are plotted in panels C and E. The inset in panel F shows a linear fit to the data for the reaction employing 40 μM A and B (violet), in comparison to the reaction with 5 μM A and B (red).

trations of A and B′ and the resulting increase in the concentrations of free A and B′ that are available to react.

Finally, the concentrations of A and B were increased simultaneously from 5 to 40 μM, while maintaining the concentrations of A′ and B′ at 5 μM (Figure 6F). This resulted in progressively decreased rates of production of E′, which can be attributed to reduced concentrations of free A′ and B′ caused by their increased level of sequestration within the nonproductive complexes. At the same time, the concentrations of free A and B progressively increased, as evidenced by the increased rate of production of E during the initial phase of the reaction (Figure 6F, inset). However, this is a linear rate of reaction because it is not supported by an increased level of production of the autocatalytic partner E′. At 40 μM A and B, the linear rate of production of E was 0.4 min^{-1}, which is close to the rate of dissociation of the E·E′ complex. This is in contrast to the behavior observed with substrate concentrations of 5 μM, at which the reaction already exhibits sigmoidicity within the first 2 h.

DISCUSSION

A kinetic framework for the self-replicating RNA enzymes can be established from the results obtained in this study. A central conclusion is that the rate of RNA-catalyzed RNA ligation is not rate-limiting for the complete replication system. The k_{cat} values for the two component ligation reactions are in the range of 2−5 min^{-1}. If these were rate-limiting, exponential amplification would occur with a doubling time of ∼20 s and would reach its maximal extent in just a few minutes. Multiple turnovers for the two component reactions are limited by the rate of dissociation of the E·E′ complex, which is ∼10-fold slower than k_{cat}. However, this too is not rate-limiting for the complete replication system. If it were, the system would not exhibit sigmoidal growth and would not proceed with a reaction order of 1.0, indicative of exponential amplification, and the

dx.doi.org/10.1021/bi301646n | Biochemistry 2013, 52, 1227−1235

reaction rate would be ~10-fold faster than the observed rate of ~0.03 min^{-1}.

The observed rate for the complete replication system is restricted by the availability of free substrates, which are present at concentrations well below the K_M of the corresponding enzyme–substrate complexes. Because of the inherent complementarity of the system, substrates A and B bind to E′ but also bind to opposing substrates B′ and A′, respectively. Similarly, A′ and B′ bind to E but also to B and A, respectively. It is the formation of the nonproductive A·B′ and A′·B complexes that reduces the availability of free substrates. The K_M values of the enzymes for their corresponding substrates are in the range of 1–8 μM, but the K_d values of the nonproductive complexes are ~0.1 μM. Thus, when substrate concentrations of 5 μM each are used, only ~10% of the substrate molecules are free in solution. As a result, the enzymes are poorly saturated and the observed rate is only ~0.03 min^{-1}. Nonetheless, exponential growth is observed because the nonproductive complexes have a fast dissociation rate (>1 min^{-1}), which continually makes substrate molecules available to bind to the enzymes.

Increasing the concentration of one of the four substrates, in excess of that of its partner in the nonproductive complex, increases the free concentration of that substrate. However, this does not increase the rate of the corresponding component reaction because the other substrate for that reaction remains limiting (Figure 6A,B). Instead, the rate of the reciprocal component reaction decreases because the elevated substrate concentration results in more complete sequestration of that substrate's partner within the nonproductive complex. If the concentrations of both substrates for the same component reaction are increased, then the rate of that reaction increases because of the enhanced saturation of the enzyme with both substrates (Figure 6F). However, the rate of the reciprocal reaction decreases because of enhanced sequestration of both of the reciprocal substrates.

The rates of the two component reactions can be increased by increasing the concentrations of both A and A′ (or both B and B′), but once saturation is reached for the enzyme–substrate complexes, there is no further benefit for the rate of exponential amplification (Figure 6C,D). Substrate concentrations substantially in excess of the K_M contribute only to the formation of nonproductive complexes. A special case arises when the concentrations are increased for both components of the same nonproductive complex (Figure 6E). This results in an increased level of sequestration of both excess substrates within the same nonproductive complex and increased free concentrations of those substrates because of the equilibrium between bound and free components. The concentration of free components increases as the square root of the increased concentration of the bound components, still contributing to enhanced saturation of both enzymes, and therefore increasing the rate of exponential amplification.

Kinetic modeling was conducted to provide a better understanding of the overall reaction system and to seek ways to improve the rate of exponential amplification. The exponential amplification profiles (Figure 2A) were fit to a model based on Figure 1B, including the nonproductive A·B′ and A′·B complexes, but not the spontaneous reaction pathway initiated by the B′·A·A′·B complex. The starting concentrations of the B and B′ substrates were adjusted for their maximal extent of reaction (see Results). The experimentally determined K_d values for the E·E′, A·B′, and A′·B complexes were used to calculate the concentrations of free and bound reactants throughout the course of amplification (see Experimental Procedures).

Figure 7 depicts the estimated concentrations of the various components over time, starting with 0.1 μM each for E and E′.

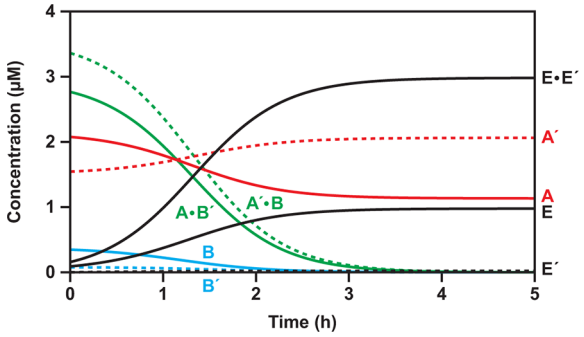

Figure 7. Estimation of the concentrations of various reaction components during the course of exponential amplification, based on the data shown in Figure 2A and the experimentally determined K_d values for the E·E′, A·B′, and A′·B complexes. The starting concentrations of A and A′ (red) were 5 μM each, the starting concentrations of B and B′ (blue), adjusted for their maximal extent of reaction, were 3.5 and 3 μM, respectively, and the starting concentrations of E and E′ (black) were 0.1 μM each. At the outset of the reaction, most of the substrates existed as A·B′ and A′·B complexes (green), with the excess A and A′ molecules remaining free in solution.

As expected, the majority of substrate molecules exist as A·B′ and A′·B complexes and the majority of enzyme molecules exist as the E·E′ complex. The overall kinetic profile is controlled by the relative equilibrium constants of the various complexes, with exponential amplification occurring at a rate of 0.034 min^{-1}.

There are several ways in which faster rates of exponential amplification might be achieved. A modest increase in k_{cat} of the two component reactions would result in a proportional increase in the observed rates of these reactions (eq 8) and in the overall rate of amplification. However, if k_{cat} were to increase by more than 7-fold, then dissociation of the E·E′ complex would become rate-limiting and the system would no longer exhibit exponential growth. The best that could achieved would be an exponential growth rate of ~0.2 min^{-1}, corresponding to a doubling time of 3 min. Faster exponential growth also would result if the K_m of the enzyme–substrate complexes were reduced relative to the K_d of the nonproductive A·B′ and A′·B complexes. This would provide more complete saturation of the enzymes for a given concentration of free substrates, contributing to faster observed rates of reaction. Again, however, the maximal rate of exponential growth would be limited by the rate of dissociation of the E·E′ complex. Faster product dissociation would allow a higher maximal rate of exponential amplification. It also would benefit the amplification rate, even without an improved k_{cat} or K_m, because it would provide higher concentrations of free E and E′ for conducting the ligation reaction.

Improved replicator designs should aim to improve the catalytic efficiency, k_{cat}/K_M, of the RNA-catalyzed reactions, within the limit set by the rate of dissociation of the E·E′ complex. This might be achieved by increasing the stability of the enzyme–substrate complexes, so long as that did not result in comparable stabilization of the A·B′ and A′·B complexes,

which rely on the same base-pairing interactions. It would be desirable, for example, to improve K_M through enhanced tertiary interactions in the region of the ligation junction, which would not pertain to the nonproductive complexes. In vitro evolution experiments are currently underway to develop self-replicating RNA enzymes with an improved k_{cat}/K_M. Such enzymes would have the added advantage of being able to operate efficiently at lower substrate concentrations, thus allowing implementation of more complex populations during self-sustained evolution and more sensitive detection of target molecules during ligand-dependent exponential amplification.

The RNA-catalyzed exponential amplification system is the only known genetic system outside of terrestrial biology. It provides a working model of biological replication and has some capacity for self-sustained Darwinian evolution. In both natural and synthetic genetic systems, replication is the primary determinant of fitness. Replication not only entails the literal duplication of the genetic material but also depends on an adequate supply of the components that support the replicative process. As this study demonstrates, when the replication machinery is starved for fuel, its performance is restricted. Genetic variants that are less subject to these restrictions would enjoy a selective advantage, exhibiting faster exponential growth rates that would allow them to outcompete others in an evolving population.

AUTHOR INFORMATION

Corresponding Author

*E-mail: gjoyce@scripps.edu. Phone: (858) 784-9844.

Funding

This work was supported by Grant NNX07AJ23G from the National Aeronautics and Space Administration and Grant R01GM065130 from the National Institutes of Health. A.C.F. was supported by a postdoctoral cross-disciplinary fellowship from the Human Frontier Science Organization.

Notes

The authors declare no competing financial interest.

REFERENCES

(1) von Kiedrowski, G. (1986) A self-replicating hexadeoxynucleotide. *Angew. Chem. 25*, 932−935.

(2) Zielinski, W. S., and Orgel, L. E. (1987) Autocatalytic synthesis of a tetranucleotide analogue. *Nature 327*, 346−347.

(3) von Kiedrowski, G., Wlotzka, B., Helbing, J., Mazten, M., and Jordan, S. (1991) Parabolic growth of a self-replicating hexadeoxynucleotide bearing a 3′-5′-phosphoamidate linkage. *Angew. Chem. 30*, 423−426.

(4) Paul, N., and Joyce, G. F. (2002) A self-replicating ligase ribozyme. *Proc. Natl. Acad. Sci. U.S.A. 99*, 12733−12740.

(5) Vaidya, N., Manapat, M. L., Chen, I. A., Xulvi-Brunet, R., Hayden, E. J., and Lehman, N. (2012) Spontaneous network formation among cooperative RNA replicators. *Nature 491*, 72−77.

(6) Lee, D. H., Granja, J. R., Martinez, J. A., Severin, K., and Ghadiri, M. R. (1996) A self-replicating peptide. *Nature 382*, 525−528.

(7) Yao, S., Ghosh, I., Zutshi, R., and Chmielewski, J. (1997) A pH-modulated, self-replicating peptide. *J. Am. Chem. Soc. 119*, 10559−10560.

(8) Rubinov, B., Wagner, N., Rapaport, H., and Ashkenasy, G. (2009) Self-replicating amphiphilic β-sheet peptides. *Angew. Chem. 48*, 6683−6686.

(9) Tjivikua, T., Ballester, P., and Rebek, J. (1990) A self-replicating system. *J. Am. Chem. Soc. 112*, 1249−1250.

(10) Terfort, A., and von Kiedrowski, G. (1992) Self-replication by condensation of 3-amino-benzamidines and 2-formylphenoxyacetic acids. *Angew. Chem. 5*, 654−656.

(11) Wang, T., Sha, R. J., Dreyfus, R., Leunissen, M. E., Maass, C., Pine, D. J., Chaikin, P. M., and Seeman, N. C. (2011) Self-replication of information-bearing nanoscale patterns. *Nature 478*, 225−228.

(12) Schulman, R., Yurke, B., and Winfree, E. (2012) Robust self-replication of combinatorial information via crystal growth and scission. *Proc. Natl. Acad. Sci. U.S.A. 109*, 6405−6410.

(13) von Kiedrowski, G. (1993) Minimal Replicator Theory I: Parabolic versus Exponential Growth. In *Bioorganic Chemistry* (Dugas, H., Ed.) Vol. 3, pp 115−146, Springer-Verlag, New York.

(14) Issac, R., and Chmielewski, J. (2002) Approaching exponential growth with a self-replicating peptide. *J. Am. Chem. Soc. 124*, 6808−6809.

(15) Rogers, J., and Joyce, G. F. (2001) The effect of cytidine on the structure and function of an RNA ligase ribozyme. *RNA 7*, 395−404.

(16) Lincoln, T. A., and Joyce, G. F. (2009) Self-sustained replication of an RNA enzyme. *Science 323*, 1229−1232.

(17) Kim, D. E., and Joyce, G. F. (2004) Cross-catalytic replication of an RNA ligase ribozyme. *Chem. Biol. 11*, 1505−1512.

(18) Sczepanski, J. T., and Joyce, G. F. (2012) Synthetic evolving systems that implement a user-specified genetic code of arbitrary design. *Chem. Biol. 19*, 1324−1332.

(19) Lam, B. J., and Joyce, G. F. (2009) Autocatalytic aptazymes enable ligand-dependent exponential amplification of RNA. *Nat. Biotechnol. 27*, 288−292.

(20) Lam, B. J., and Joyce, G. F. (2011) An isothermal system that couples ligand-dependent catalysis to ligand-independent exponential amplification. *J. Am. Chem. Soc. 133*, 3191−3197.

(21) Pluthero, F. G. (1993) Rapid purification of high-activity *Taq* DNA polymerase. *Nucleic Acids Res. 21*, 4850−4851.

(22) Ellinger, T., and Ehricht, R. (1998) Single-step purification of T7 RNA polymerase with a 6-histidine tag. *BioTechniques 24*, 718−720.

(23) Forster, A. C., and Altman, S. (1990) External guide sequences for an RNA enzyme. *Science 249*, 783−786.

(24) Olea, C., Jr., Horning, D. P., and Joyce, G. F. (2012) Ligand-dependent exponential amplification of a self-replicating L-RNA enzyme. *J. Am. Chem. Soc. 134*, 8050−8053.

(25) Pleiss, J. A., Derrick, M. L., and Uhlenbeck, O. C. (1998) T7 RNA polymerase produces 5′ end heterogeneity during *in vitro* transcription from certain templates. *RNA 4*, 1313−1317.

(26) Helm, M., Brulé, H., Giegé, R., and Florentz, C. (1999) More mistakes by T7 RNA polymerase at the 5′ ends of *in vitro*-transcribed RNAs. *RNA 5*, 618−621.

(27) Nelson, J. W., and Tinoco, I. (1982) Comparison of the kinetics of ribo-, deoxyribo- and hybrid oligonucleotide double-strand formation by temperature-jump kinetics. *Biochemistry 21*, 5289−5295.

(28) Santoro, S. W., and Joyce, G. F. (1998) Mechanism and utility of an RNA-cleaving DNA enzyme. *Biochemistry 37*, 13330−13342.